Vol. 13, No. 35, summer 2023, pages 31-38

Journal of Analytical and Numerical Methods in Mining Engineering

Journal home page: http://anm.yazd.ac.ir/

Research article

Numerical modeling of the effect of Anderson's stress regimes on the volume of sand production in oil wellbores

Abolfazl Abdollahipour[1*], Alireza Kargar[1], Mohammad Fatehi Marji[2]

1- Dept. of Mining Engineering, College of Engineering, University of Tehran, Tehran, Iran
2- Dept. of Mining and Metallurgy Engineering, Yazd University, Yazd, Iran

*Corresponding author: E-mail: *Abdollahipour@ut.ac.ir*
(Received: *November 2022*, Accepted: *April 2023)*

DOI: 10.22034/ANM.2023.19302.1580

Keywords

Sand Production
Material Erosion
3D Finite Element Model
Stress Regimes
Drawdown Pressure

Abstract

Sand production is a complex mechanism that reduces oil and gas production and leads to wellbore instability, tubing erosion, and even erosion of surface installations. The hydrodynamic action of the flow on the surface leads to the breakup of solid particles from the surface. This is one of the main sources of sand production. The sand production may be affected by the combination of flow rate and the stress regime around the wellbore. In this paper, sand production in a vertical wellbore is numerically studied. A 3D finite element model in various stress regimes (i.e., normal, strike-slip, and reverse based on Anderson's classification) presenting various conditions of reservoirs was used. A typical drawdown pressure was chosen to simulate the production in the wellbore. The numerical model uses a sand production criterion based on the velocity of the fluid flow, the porosity of formation, transport concentration, and sand production coefficient to determine the initiation of sand production. The sand production volume was determined for a duration of a week in all cases. The most erosion of materials in all models occurred near the junction of the wellbore and perforation. This is an expected result since based on rock mechanics, the junction of the wellbore and perforation is also the location of the most stress concentration. It was concluded that the collaboration of high-stress concentration and high-pressure drawdown caused the excessive sanding problem. The results of the paper provide insight into the effect of stress regimes and orientation of perforation on the volume of sand production.

1. INTRODUCTION

The optimization of wellbore stability and oil or natural gas production may be considered as a balance among the recovery rate, the sustainability of the recovery, and the cost of operating the well. This balance requires controlling sand production; a problem in oil and natural gas fields when they are extracted under sufficiently high pressure. Sand production in poorly consolidated reservoirs is one of the main problems of oil and gas industries since the beginning of the commercial production of oil and natural gas. More than 70% of hydrocarbon reservoirs in the world are affected by sand production. The sand accumulation in the well or its movement to the surface mostly depends on the flow velocities. The accumulated sand affects the recovery sustainability while its movement to the surface along with the hydrocarbon results in the erosion of the piping system and its components. More than 70% of the worldwide reservoirs are located in weakly consolidated

formations which are prone to sand production and wellbore stability problems [1]–[5]. On the other hand, controllable sand production may increase wellbore productivity and reduce wellbore completion costs [6]. The expensive costs of sand production control and its wide impact on the production life of a well, have made this phenomenon focus of much research.

There are several controlling systems for sand production prevention. It can be prevented before the initiation of wellbore production by the installation of downhole sand control systems such as gravel packs, and sand screens. Furthermore, chemical consolidations can inhibit the movement of sand into the underground and surface facilities. With no sanding prevention systems, the conventional sand management approach is to reduce the hydrocarbon production rate to minimize the produced sand. However, this can significantly reduce wellbore productivity. On the other hand, sand production increases the porosity and permeability close to the wellbore which results in a greater flow of liquid into the wellbore[7]–[9]. There have been many studies to better understand sand production and to determine its most influential parameters. Several studies have tried to experimentally simulate this phenomenon in laboratories [10]–[14]. Wu et al. [15] studied seven various weak sandstones in the lab. The experimental results suggested a shear failure mechanism around the borehole. The failure was followed by erosion of the loose materials due to flowing fluid in the failure zone. Others have interpreted field data and proposed empirical relations for sand production [16], [17]. Ghalambor et al. statistically studied sand production in gas wells. They showed that a project can be optimized when sand control decisions are made at the time of initial completion. There are also many studies concerned with developing theoretical [18]–[21] and numerical [22]–[26] models for a better presentation of sand production and similar problems n wellbores [26]–[31]. Risnes et al. investigated the stresses around the wellbore using the elastic-plastic Mohr-Coulomb theory. Geertsma studied some geomechanical aspects of well completions and sand production in wells during injection and production. Abdollahipour et al. proposed a thermo-hydromechanical boundary element model to take into account the effect of hydraulic and thermal effects on wellbore stability [26]. Khamitov et al. investigated sand production using the coupled DEM/CFD model. They determined the porosity distribution around the perforation hole [22].

The correct prediction of sand production volume can significantly reduce production costs by decreasing the chance of wellbore failure and erosion of surface facilities which may occur during sand production. Previous studies have not specifically studied the effect of various stress regimes on sand production. Therefore, this topic requires further investigation. In this study, a fully 3D finite element model using ABAQUS software is developed to study the effect of various stress regimes on sand production in a hypothetical well. Although the FEM requires more computational power than FDM, it has higher accuracy than the FDM. In comparison to the BEM, there is no need for an analytical solution for solving unknowns in the FEM. The volume of sand production in three stress regimes based on Anderson's classification is studied.

2. RESEARCH METHODOLOGY

2.1. Modeling Assumptions

Generally, the main sources of sand production are poor rock strength and operational/production conditions. It can be due to the geological condition/structure of the reservoir sand. Therefore, the following forces may impact sand production [27]:

- Cementing materials that bond the sand grains together.
- Friction between the sand grains coupled with compressive stresses that result in the formation of naturally stable arches.
- Cohesion (capillary forces) due to a common fluid phase wetting the sand grains.

Two main sources contribute to sand production in a wellbore. One of the sources is the existence of high stresses near wellbores and perforations. Stresses higher than the rock's strength lead to rock failure. Solid particles i.e., sands break up and are transported by the fluid through the pores. The other source is the hydrodynamic action of the flow on the surface which also breaks up the particles from the surface. The dominant cause of sand production is determined by the properties of the reservoir rock and the flow velocities. Fig. 1 shows 3 stages of sand production; Onset, transient sanding, and steady-state sanding.

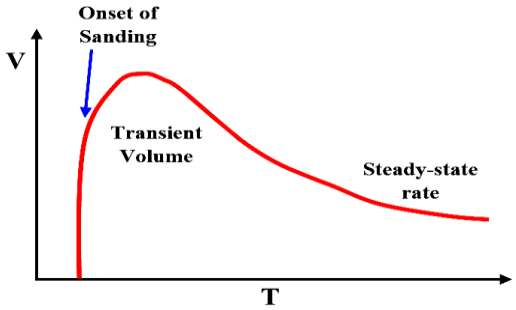

Fig. 1. Sand production stages as a function of time (redrawn from [28]).

In this paper, an erosion equation based on the theoretical model proposed by Van den Hoek et al. [14] is used. The method is more focused on the second source of sand production (i.e. hydrodynamic source). However, its similarity with the equation of Papamichos and Stavropoulou [18] helps to approximate the first source of sand production as well. This is due to the fact that high stresses caused by stress concentration appear only in a close perimeter of the wellbore. The evolution of the localized deformation is combined with the effect of hydrodynamic erosion in the equation of Papamichos and Stavropoulou. The sand production equation is [14].

$$V_e = \xi(1-n)cv_w \quad (1)$$

where V_e is the sand production velocity, v_w is the velocity of pore fluid, c is the transport concentration, n is the lagrangian porosity, and ξ is the sand production coefficient. ξ is based on the equivalent plastic strain $\bar{\varepsilon}^{pl}$. This coefficient is equal to and is constrained by a constant ξ_2. it is also equal to zero when a cutoff equivalent plastic strain is passed.

ξ_1 and ξ_2 both must be experimentally determined. In this paper $\bar{\varepsilon}^{pl}_{cutoff} = 0.028$, $\xi_1 = 4$, $\xi_2 = 0.01$. A transport concentration c = 0.001 as recommended by Papamichos and Stavropoulo is used. The values are deliberately determined in a way to show a tangible erosion in a limited analysis time.

Sand production initiates when the sand production velocity V_e exceeds the value provided by Eq. (1) in any node of the FEM. In other words, Eq. (1) describes a critical erosion velocity as a function of solution quantities i.e., v_w, c, ξ and n. The adaptive meshing capability of ABAQUS provides a conduit for calculating V_e, while at the same time keeping its progression normal to the moving surface of the eroded material. This capability also adjusts subsurface nodes to account for large amounts of erosive material loss [29]

A 3D finite element model of a vertical wellbore with four perforations (i.e. 90° phase angles) is developed in ABAQUS. Due to symmetry, only one-fourth of the geometry (a quarter of the well and one perforation) shown in Fig. 2 is modeled to reduce the computation time. Fig. 2 shows the initial geometry of the well and perforations. To avoid boundary effects, a domain of almost 35 ft. has been modeled.

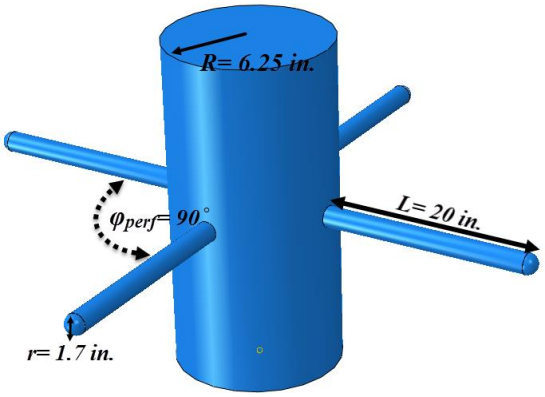

Fig. 2. Initial geometry of the wellbore and perforations.

The model is brought to initial equilibrium through a geostatic step, where initial stress and initial pore pressure are applied. In the next step, excavation of the wellbore and the perforation tunnel is simulated by removing the materials occupying their place. And finally, the sand production is modeled for a duration of a week. An adaptive meshing technique is used to simulate erosion of the material surface.

Mesh velocities computed by the meshing algorithm are modified to account for the computed erosion velocities at each node. Then, using Eq. (1), the modified velocities are calculated [29].

2.2 Adaptive Re-Meshing Technique

Sand production is simulated by the erosion of surface materials at the final step of iteration for each analysis. The erosion equation determines the critical velocity required for the initiation of material erosion as a function of several solution quantities. The adaptive re-meshing technique provides the necessary tools for calculating this surface velocity and at the same time keeping its progression normal to the surface of the moving eroded surface. The subsurface nodes adjust to account for large material loss due to erosion.

A spatial adaptive re-meshing technique is used to model erosion. The technique is used for

all the nodes on the surface of the perforation. It should be noted that the adaptive mesh constraints can be used only on adaptive mesh domains. Therefore, an appropriate extent of the finite element mesh near the surfaces of the wellbore and perforation tunnels is considered the adaptive mesh domain.

The numerical procedure used for this study is widely tested, applied, and validated in the literature [29] and we will not try to revalidate the FEM procedure. Furthermore, the applied model for studying sand production is also well-established in several papers and will not require validation [2], [14], [18], [2].

2.3. Stresses And Geomechanical Properties

To study the effect of different in situ stress regimes, sand production is modeled in (total) stress regimes defined by Anderson's classification scheme according to Table 1. Also, the reservoir pore pressure of 4500 psi was considered in all numerical models, unless told otherwise. Fig. 3 shows boundary conditions for all models in a 2D model for simplicity. Vertical stress is in the out-of-plane direction which is not shown in the figure. It should be noted that since only a quarter of the wellbore is modeled, displacement boundary was applied on symmetry planes. The production pressure was used as a hydraulic boundary condition on the wellbore wall and perforation tunnels. 1144 quadrilateral linear elements of M3D4 and 14352 hexahedral linear elements of C3D8P were used to model the problem.

Table 1. Relative stress magnitudes in Anderson's classification scheme

Regime	Stress (psi)		
	σ_1=10000	σ_2=7500	σ_3=7000
Normal	σ_V	σ_H	σ_h
Strike-slip	σ_H	σ_V	σ_h
Reverse	σ_H	σ_h	σ_V

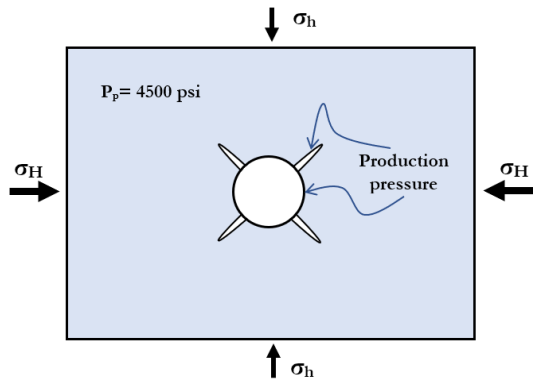

Fig. 3. Boundary conditions for all models in a simplified 2D model (vertical stress (σ_v) is in out of plane direction).

The Drucker-Prager is considered for the host rock since it considers the effect of middle principal stress too and also is widely used for consolidation analysis of sandstones. Table 2 shows the properties used for the Drucker-Prager criterion.

Table 2. Drucker-Prager properties of the rock

φ(°)	K	ψ(°)	E(psi)	ν
45	0.8	40	10^6	0.25

Where φ is the internal friction angle, K is the ratio of the flow stress in triaxial tension to the flow stress in triaxial compression ($0.778 \le K \le 1.0$), and ψ is the dilation angle.

In many studies, permeability is defined as a function of porosity. The following relation between porosity and permeability was considered in this study [30]

$$k = \frac{-1.036 \times 10^{-4} n}{-3.061 \times 10^{-1} + n} \qquad (2)$$

where n is porosity and k is permeability in in./s. The average permeability and porosity of the host rock were 5.79×10^{-4} in./s and 26% respectively.

3. NUMERICAL MODELING RESULTS AND DISCUSSION

Three numerical models based on the assumptions and input parameters described in the previous section were built. Fig. 4 shows the perforation and a quarter of the wellbore modeled in this study.

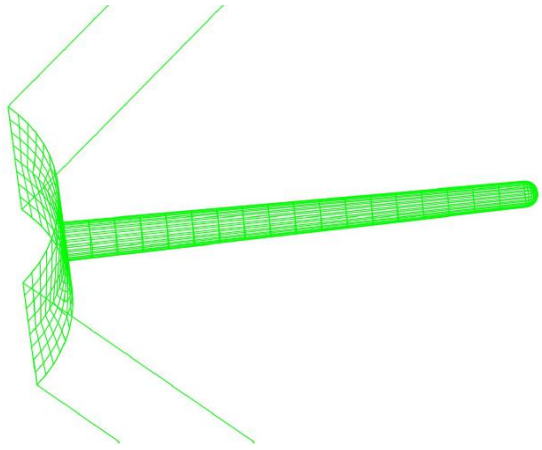

Fig. 4. Perforation tunnel and wellbore intersection considered in this study.

Fig. 5 shows Mises (effective) stress distribution in models after 7 days of production. As can be seen in Fig. 5(a), a higher state of stress exists in relation to Fig. 5(b) and (c). Stress concentration around the perforation tunnel in a

normal stress regime is more than 6000 psi in sidewalls and less than 1000 psi in the crown and bottom. This is due to high vertical stress and low horizontal stress acting perpendicular to the perforation wall. A low-stress distribution is also visible around the wellbore in Fig. 5 (a). Lower stress concentrations exist around the perforation and tunnels of Fig. 5 (b) and (c). Stress concentration around the wellbore in the strike-slip regime is quite high in some parts which is again due to the high difference between principal stresses (σ_h and σ_H equal to 7000 psi and 10000 psi respectively) perpendicular to its walls. These results show that a normal stress regime may prove to be the most critical situation in sand production.

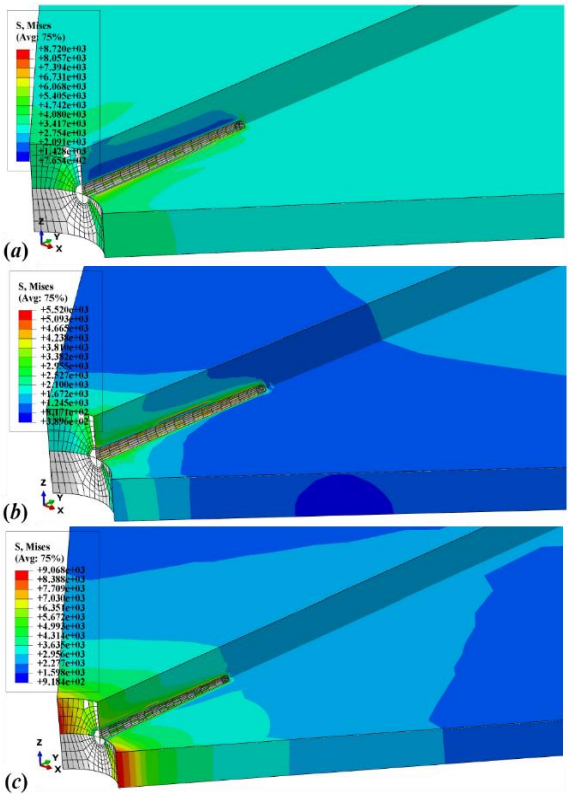

Fig. 5. Mises (effective) stress distribution after 7 days of production at production pressure of 4000 psi a) Normal faulting regime, b) Reverse faulting regime, c) Strike-slip faulting regimes.

Fig. 6 demonstrates the pore pressure distribution after 7 days of production. A section of perforation is exhibited using two plane cuts to show pore pressure distribution around the perforation tunnel as well. The pore pressure distribution is identical in all stress regimes since it is based on initial pore pressure and drawdown pressure which are constant in all stress regimes. As can be seen, pore pressure in the far field is equal to the initial pore pressure and lower pore pressures are available around the perforation tunnel and wellbore due to production.

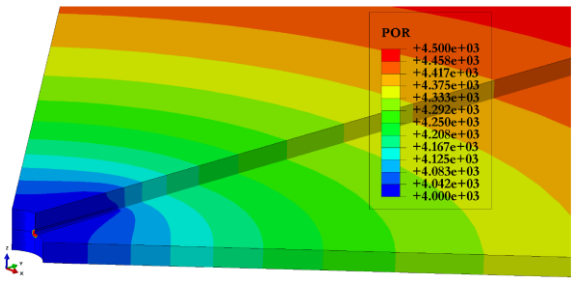

Fig. 6. Pore pressure distribution after 7 days of production at a production pressure of 4000 psi.

Fig. 7 presents equivalent plastic strain at the intersection of the wellbore wall and perforation tunnel. An almost uniform distribution is reached in Fig. 7 (c) for the strike-slip stress regime. However, Fig. 7 (a) (and to a less degree Fig. 7 (b)) shows a concentration of plastic strain in both sidewalls of the perforation tunnel. It is an indication of a probable higher tendency towards erosion in these areas. Fig. 8 (a) shows equivalent plastic strain (PEEQ) immediately after excavation of perforation tunnels and Fig. 8 (b) shows PEEQ after total 7 days of production in a normal stress regime. An increase in plastic strain is evident after the initiation of production in this perforation tunnel. Since erosion in these models is not significant (See Fig. 9), a tangible change in the cross-section area has not occurred.

Fig. 9 shows the volume of sand production in each model after a week of production under the pressure of 4000 psi (i.e. $\Delta P=P_{reservoir}-P_{well}=500$ psi). Sand production was similar in all stress regimes. A higher sanding was observed in the case of the normal stress regime and a lower rate of sand production may be seen in Fig. 7 for the strike-slip regime. It should be noted that the reported sand volumes are produced from only one perforation in a quarter of a full model. Hence, the total sand production from this section of the well must be multiplied by 4. Total sand production in all lengths of the well must consider all perforations which may rise to 100s of perforations, resulting in a 100sfold increase in sand production. These sand productions are obtained while considering a very reasonable (and maybe a bit low) drawdown pressure. The steady-state (and low) sand production after a week, shows a stable sanding condition for the wellbore with the current design. However, the decision of using this design should be achieved after considering total sand production from all perforations and investigating if the current production rate is adequate.

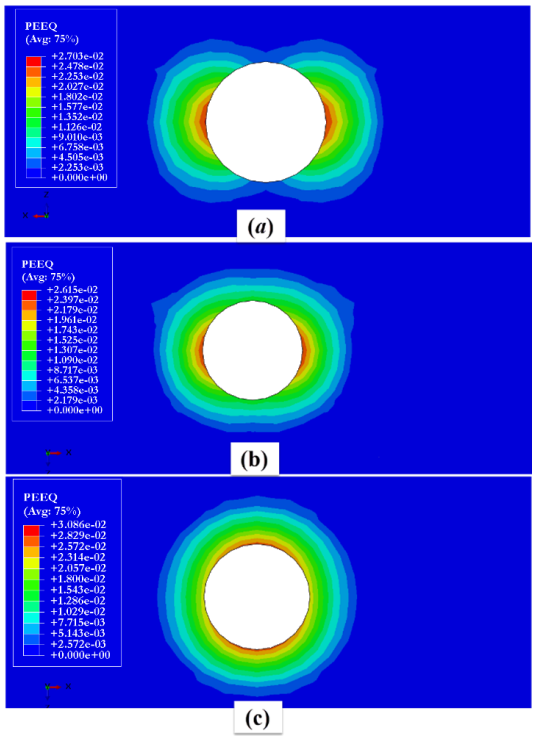

Fig. 7. Equivalent plastic strain distribution around the intersection of the wellbore and the perforation tunnel at a production pressure of 4000 psi.

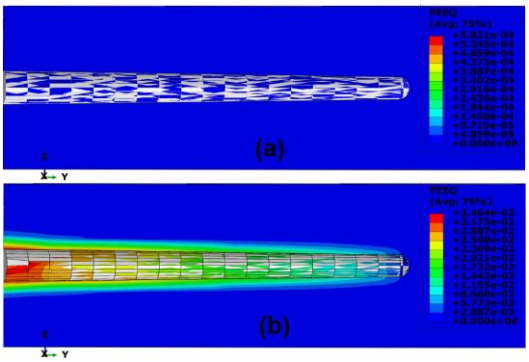

Fig. 8. Equivalent plastic strain distribution around a perforation tunnel (a) before production, (b) after production.

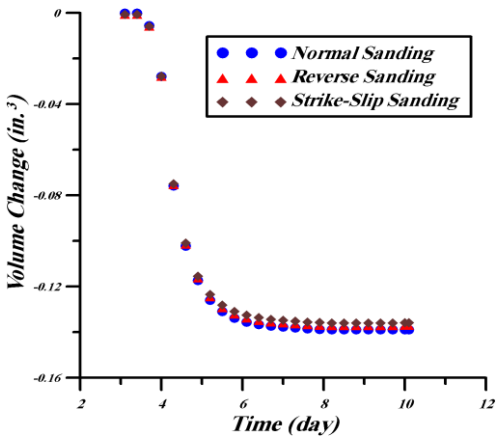

Fig. 9. Volume of sand production after 7 days of production at a drawdown pressure of 4000 psi.

To further investigate the assumption made in Fig. 6 (higher sand production in normal stress regime in sidewalls of perforation tunnel) another set of models was run considering a higher drawdown pressure value. A production pressure of 3000 psi (i.e. $\Delta P = P_{reservoir} - P_{well} = 1500$ psi) was considered. As shown in Fig. 10 the volume of sand production is significantly increased for the normal stress regime.

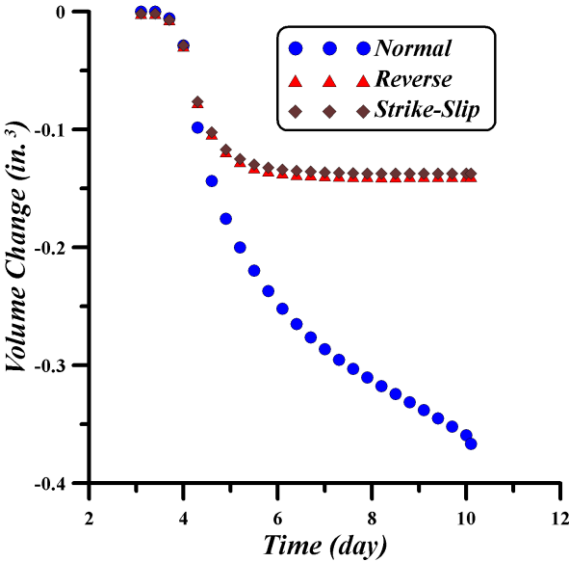

Fig. 10. Volume of sand production after 7 days of production with an exaggerated drawdown pressure.

Fig. 11 shows the deformation (i.e. due to erosion) of the intersection of the wellbore and perforation tunnel. As expected from Fig. 7 (a), most sand production has occurred in the side walls of the perforation tunnel of the normal stress regime. The shape has dramatically altered due to excessive sanding during a week of oil production in a normal stress regime (Fig. 11 (a)). Fig. 11 (b) and (c) show negligible deformation and plastic strain around the perforation intersection with the wellbore. The main reasons for significant sand production in normal stress regimes in these models are very high-stress concentration and high-pressure drawdown. The high-stress concentration weakens rock formation preparing it for separation from the wellbore surface and high-pressure drawdown helps with the hydrodynamic action of the flow on the surface. The collaboration of these two main sources of sand production has resulted in the observed sand production in normal stress regimes.

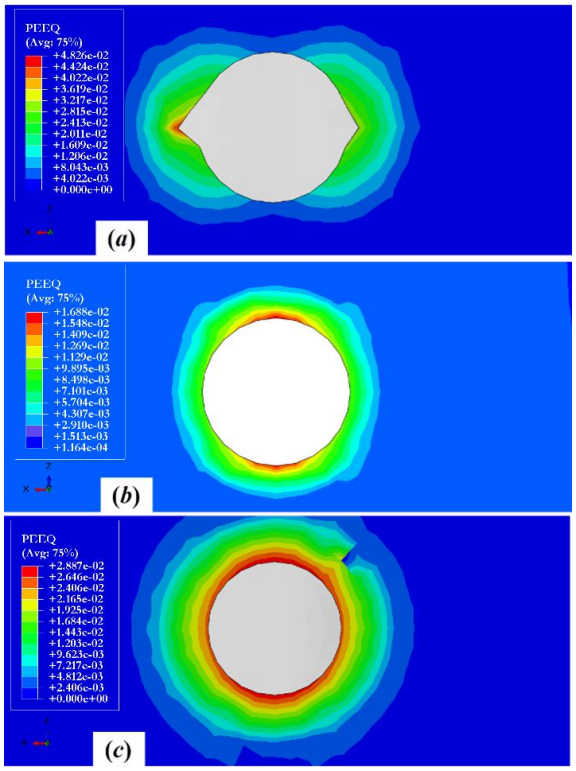

Fig. 11. Equivalent plastic strain distribution around the intersection of the wellbore and the perforation tunnel after 7 days at production pressure of 3000 psi a) Normal stress regime, b) Reverse stress regime, c) Strike-slip stress regime.

Although a high-pressure drawdown was considered in the second set of numerical modeling, reverse and strike-slip regimes did not exhibit significant sand production. This was due to the fact that the lack of stress concentration in these models eliminated one of the sources of the sanding problem resulting in a steady state.

4. CONCLUSIONS

Sand production as one of the problems in the production stage of a wellbore was studied. A 3D finite element model was built to study the volume of sand production in a wellbore and a perforation emanated from it (a quarter of the whole model). Three different stress regimes according to Anderson's classification were considered. Results showed that the maximum sand production occurred at the normal faulting regime while other regimes exhibited insignificant sand production. Also, the rate of sand production was derived for all models. Another set of models was run for a production pressure of 3000 psi (i.e., ΔP=1500 psi). This resulted in an unstable sand production rate in a normal stress regime. The sanding rate after a week of production showed that many problems may occur if such a production pressure and stress regime are met in a model.

A decision on working with the current sand production rate should be made based on the requirements of the wellbore performance and acceptable sand volume that can be handled by the surface equipment.

It was also shown that for significant sand production, both sources of sanding i.e., high stresses near wellbore and perforations, and hydrodynamic action of the flow on the surface are needed. In this study, the absence of the first source in reverse and strike-slip regimes prohibited significant sand production.

5. ACKNOWLEDGEMENTS

The authors acknowledge the financial support from Iran National Science Foundation (INSF), Tehran, and Yazd University research affairs (research project INSF-YAZD 96010905).

REFERENCES

[1] J. Bellarby, "Well completion design," in Paper presented at Developments in Petroleum Science, 2009.

[2] A. Nouri, H. Vaziri, H. Belhaj, and R. Islam, "Sand-production prediction: a new set of criteria for modeling based on large-scale transient experiments and numerical investigation," SPE Journal, vol. 11, no. 9, p. 26e9, 2006.

[3] I. C. Walton, D. C. Atwood, P. M. Halleck, and C. B. Bianco, "Perforating unconsolidated sands: an experimental and theoretical investigation," SPE Drilling Completion J, vol. 17, no. 3, pp. 141–150, 2002.

[4] H. Yousefian et al., "Numerical simulation of a wellbore stability in an Iranian oilfield utilizing core data," J Pet Sci Eng, vol. 168, pp. 577–592, Sep. 2018.

[5] A. Abdollahipour, M. Fatehi-Marji, A. Yarahmadi-Bafghi, and J. Gholamnejad, "A Fourth Order Formulation of DDM for Crack Analysis in Brittle Solids," Analytical and Numerical Methods in Mining Engineering, vol. 3, no. 6, 2016.

[6] R. J. J. Saucier, "Considerations in Gravel Pack Design," J Pet Technol, vol. 26, no. 2, 1974.

[7] P. R. Gunjal, V. v. Ranade, and R. v. Chaudhari, "Computational study of a single-phase flow in packed beds of spheres," AIChE Journal, vol. 51, no. 2, pp. 365–378, Feb. 2005, doi: 10.1002/AIC.10314.

[8] Y. Q. Feng and A. B. Yu, "Assessment of model formulations in the discrete particle simulation of gas-solid flow," Ind Eng Chem Res, vol. 43, no. 26, pp. 8378–8390, Dec. 2004, doi: 10.1021/IE049387V.

[9] S. Chen and G. D. Doolen, "Lattice boltzmann method for fluid flows," Annu Rev Fluid Mech, vol. 30, pp. 329–364, 1998, doi: 10.1146/ANNUREV.FLUID.30.1.329.

[10] V. Fattahpour, M. Moosavi, and M. Mehranpour, "An experimental investigation on the

effect of rock strength and perforation size on sand production," J. Pet. Sci. Eng., vol. 86–87, 2012.

[11] C. D. Hall and W. H. Harrisberger, "Stability of sand arches: a key to sand control," J. Pet. Technol., vol. 22, pp. 821–829, 1970.

[12] A. Kooijman, P. Halleck, D. Philippus, C. Veeken, and C. Kenter, "Large-scale laboratory sand production test," in SPE Annual Technical Conference and Exhibition, 1992.

[13] D. Tippie and C. Kohlhaas, "Effect of flow rate on stability of unconsolidated producing sands," in Fall Meeting of the Society of Petroleum Engineers, 1973.

[14] P. Van den Hoek, G. Hertogh, A. Kooijman, P. De Bree, C. Kenter, and E. Papamichos, "A new concept of sand production prediction: theory and laboratory experiments," SPE Drilling Completion J., vol. 15, 2000.

[15] B. Wu et al., "A New and Practical Model for Amount and Rate of Sand Production Estimation," in Day 3 Thu, March 24, 2016, Mar. 2016. doi: 10.4043/26508-MS.

[16] A. Ghalambor, A. Hayatdavoudi, C. Alcocer, and R. Koliba, "Predicting sand production in US Gulf coast gas wells producing free water," J. Pet. Technol., vol. 41, pp. 1336–1343, 1989.

[17] N. Stein and D. W. Hilchie, "Estimating the maximum production rate possible from friable sandstones without using sand control," J. Pet. Technol., vol. 24, pp. 1157–1160, 1972.

[18] E. Papamichos and M. Stavropoulou, "An erosion-mechanical model for sand production rate prediction," Int. J. Rock Mech. Min. Sci. Geomech. Abstr., vol. 35, pp. 531–532, 1998.

[19] Y. Wang and E. Papamichos, "Conductive Heat Flow and Thermally Induced Fluid Flow around a Well Bore in a Poroelastic Medium," Water Resour Res, vol. 30, no. 12, pp. 3375–3384, 1994.

[20] E. Papamichos, I. Vardoulakis, J. Tronvoll, and A. Skjaerstein, "Volumetric sand production model and experiment," Int. J. Numer. Anal. Methods Geomech., vol. 25, 2001.

[21] J. Geertsma, "Some Rock-Mechanical Aspects of Oil and Gas Well Completions," Society of Petroleum Engineers Journal, vol. 25, no. 06, pp. 848–856, Dec. 1985, doi: 10.2118/8073-PA.

[22] F. Khamitov, N. H. Minh, and Y. Zhao, "Coupled CFD–DEM numerical modelling of perforation damage and sand production in weak sandstone formation," Geomechanics for Energy and the Environment, vol. 28, p. 100255, Dec. 2021, doi: 10.1016/j.gete.2021.100255.

[23] N. Morita, D. Whitfill, I. Massie, and T. Knudsen, "Realistic sand-production prediction: numerical approach," SPE Prod. Eng., vol. 4, pp. 15–24, 1989.

[24] J. Ostojic, R. Rezaee, and H. Bahrami, "Production performance of hydraulic fractures in tight gas sands, a numerical simulation approach," J Pet Sci Eng, vol. 88–89, pp. 75–81, Jun. 2012, doi: 10.1016/j.petrol.2011.11.002.

[25] Y. Han and P. Cundall, "Verification of two dimensional LBM-DEM coupling approach and its application in modeling episodic sand production in borehole," Petroleum, vol. 3, no. 2, pp. 179–189, 2017.

[26] A. Abdollahipour and M. Fatehi-Marji, "A thermo-hydromechanical displacement discontinuity method to model fractures in high-pressure, high-temperature environments," Renewable Energye, vol. 153, pp. 1488–1503, 2020.

[27] B. Oyeneyen, "CH. 3: Fundamental Principles of Management of Reservoirs with Sanding Problems," in Integrated Sand Management For Effective Hydrocarbon Flow Assurance, 2015, p. 208.

[28] I. Palmer, H. Vaziri, S. Willson, Z. Moschovidis, J. Cameron, and I. Ispas, "Predicting and managing sand production: a new strategy," in SPE Annual Technical Conference and Exhibition, 2003.

[29] D. S. Simulia, "Abaqus documentation," 2016.

[30] J. Hommel, E. Coltman, and H. Class, "Porosity–Permeability Relations for Evolving Pore Space: A Review with a Focus on (Bio-)geochemically Altered Porous Media," Transp Porous Media, vol. 124, no. 2, pp. 589–629, Sep. 2018, doi: 10.1007/s11242-018-1086-2.